Volume 10, Issue 2
April 2021

ITEE Journal
Information Technology & Electrical Engineering

ISSN: - 2306-708X

Generalized Method for an Appropriate Choice of Pole Number Combinations for Brushless Doubly-Fed Machines

Kendeg Onla Clement Junior

Department of Physics, Faculty of Science, University of Ngaoundere, Cameroon

E-mail : kclementjunior@yahoo.fr

ABSTRACT

The Brushless Doubly-Fed Machines (BDFM) could become the third generation of electric machines using as a generator in wind turbines. Brushless Doubly-Fed Machines operate in variable speed with a power converter rated only for a fraction of the total power output of the machine. Contrary to Doubly Fed Induction Machines (DFIM), the Brushless Doubly-Fed Machines are more robust since there are no brushes, no slip rings and the maintenance cost of the machine is reduced. The main drawback of brushless dual-feed machines is the complexity of the magnetic interaction between the power winding magnetic field (PW) and the control winding magnetic field (CW) of the stator because they have a different number of pole pairs and the process of defining the optimal number of poles for these machines is not yet well established. The paper proposes a generalized method that allows an appropriate choice of the number of pole pairs of the power winding pp and the number of pole pairs of the control winding pc of the BDFM according to several factors. The proposed generalized method is then successfully applied for the choice of pole pairs combinations of the biggest Brushless Doubly-Fed Machines project of 20 Megawatts for wind power generation.

Keywords: *Brushless Doubly-Fed Machine (BDFM), cross-coupling, number of pole pairs of the control winding, number of pole pairs of the power winding, power converter*.

1. INTRODUCTION

Nowadays, the most popular use of Doubly-Fed Induction Machines (DFIMs) concerns Wind Power Applications. They have been preferred over the conventional squirrel-cage induction machines because those latter used as Adjustable Speed Drives (ASDs), are fully-fed machines. Indeed, all their power passes through a power converter. This has implications on the size and the total cost of the system. Doubly-fed induction machines in contrary to SCIM can operate with a converter of lower rating than its full kVA, thus offering a relative inexpensive and compact solution.

The drawback of this machine is the presence of slip-rings and brush-gear arrangement that makes it subject to frequent maintenance that can be the potential cause of sparking. These factors have been an impediment towards the wide-scale use of the DFIMs in offshore wind turbines and other various drives application [1].

To overcome this drawback, the Brushless Doubly-Fed Machine (BDFM) has been proposed in the literature as an alternative to DFIM. The BDFM offers a reliable solution without compromising the advantages of the DFIM [2]. In other words, the machine still requires a power converter of the similar rating as a DFIM, albeit freed from slip-ring and brush configuration.

The idea of the BDFM originated in the 20th century from Siemens Brothers and Lydall in 1902 [3]. In the 1910s the principles of self-cascaded machines were established where two induction machines sharing the same shaft was studied by Hunt [4]-[5] and Creedy [6]. In Broadway et al. [7]-[9] researched the concept of the BDFM was about bringing the two stators together in a single iron frame. They were also the first to investigate a salient pole rotor leading of the birth of the BDFRM.

Nowadays, the BDFM became more and more attractive as a variable speed generator as only a fractional converter is required. The use of the machine as a generator in wind turbines was first proposed by [10] and the interest that followed has been primarily focused on this application [11]-[12]. The machine has also been considered for drive applications [13]. The absence of brush gear offers the advantage of lower maintenance compared to conventional slip-ring induction generator. From [14], the BDFM should lead to a system with higher reliability.

Various BDFMs have been reported in the literature. Some of them have been designed specifically for wind power applications [11]-[15] whereas others have been primarily research tools [16]-[17]. A particular attention has been given to some aspects of BDFM design [18]- [20]. Despite the efforts made it still remains a need for a deeper understanding of the design of a BDFM.

In the design of these machines, the first step is to select the number of poles of the two stator windings to achieve the desired speed. All the reported BDFMs to date have been of the $p_p + p_c$, or cumulative type. However, as referenced by [21], $p_p - p_c$ the form or differential type of BDFM being also possible.

The task becomes more complicated when it comes to a combination of speed, output torque, and magnetization consideration to select the ideal number of poles. A further factor is the cross-coupling. The authors have always used the lower pole winding as the power winding. However, the rotor frequency being higher in this configuration, it has been

Volume 10, Issue 2
April 2021

ITEE Journal
Information Technology & Electrical Engineering

ISSN: - 2306-708X

suggested to use the higher pole winding as the power winding [22].

Considering the above reasons and the following two constraints: - there should not be any direct coupling between the two stators windings. - choosing pole pairs combinations that differ by one leads to unbalanced magnet pull. We propose in this paper a generalized method for an appropriate choice of the number of pole pairs combinations as a function of several factors like: rating of the power converter, the cross-coupling capability, mechanical speed to avoid etc.

2. BRUSHLESS DOUBLY-FED MACHINE: BDFM

2.1. Description of the BDFM

The stator of the Brushless Doubly-Fed Induction Machine has two windings, commonly referred to as the Power Winding (PW) and the Control Winding (CW). The power winding is connected directly to the grid and has a fixed voltage and frequency. On the other hand, the control winding is fed from the grid via a converter, with variable frequency and variable voltage output. PW and CW are wound with different number of pole pairs so that there is no direct coupling between the two. However, cross coupling between the two windings occurs via a special rotor.

Conceptually, the BDFM is comparable to two induction machines with different numbers of poles (different synchronous speeds for the same frequency) with rotors that are physically and electrically connected to each other. But when we observe the physical form of the machine, it resembles the self-cascade machine proposed by [4], but the difference can be observed at the power supply (the BDFM has a double power supply).

This combination of induction machines is similar to the conventional cascade connection of induction machines. Traditionally, in a cascade connection, slip rings were used to connect a machine's rotor to the next stator.

However [4], it was found that if the two machines were on the same chassis, it was advantageous to connect the rotors together, rather than connecting the stator of one machine to another rotor, thus eliminating the need for slip rings.

2.2. Classification of BDFMs

Different types of BDFMs can be found in the literature depending on the shape of their rotors. There is no direct magnetic coupling between PW and CW. A special rotor is used for magnetic coupling. Indeed, the stator and rotor windings are cross-coupled. Several types of rotors have been proposed to provide a magnetic cross-coupling as shown in Fig. 1. Three different kinds of rotors are currently under investigation: reluctance rotors, induction rotors (wound and cage rotors) and hybrid rotors.

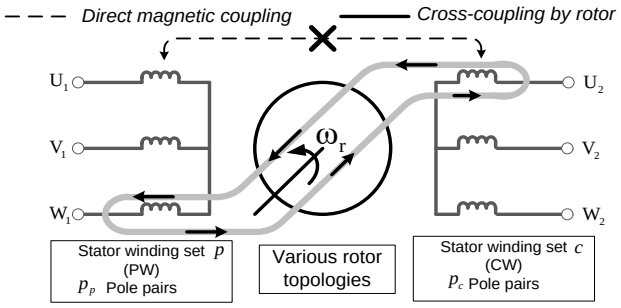

Figure 1. The schematic diagram of the BDFM.

Reluctance rotor

Compared to brushless doubly-fed machines with wound rotors and cage rotors, brushless doubly-fed reluctance machines (BDFRMs) have slightly different operating principles. The reluctance rotors change the distribution of the air-gap permeance to achieve the magnetic cross-coupling between the PW and the CW. There are three types of reluctance rotors: the reluctance rotor with simple salient poles, the segment reluctance rotor with magnetic barriers and the axially laminated anisotropic (ALA) reluctance rotor. Compared to the cage rotors, the reluctance rotors give a more effective capability of cross-coupling [23]. It can also be seen that the ALA reluctance rotor has a better synchronous operation and doubly-fed adjustable speed performance while the cage rotor gives better starting and asynchronous characteristics [24]. Moreover, recent advances have shown that brushless DFRMs with better designs can operate at high torque density and efficiency [25]-[26]. Therefore, brushless DFRMs can be potential alternatives to brushless DFIMs for wind turbine applications [2], [27].

Induction rotor

Compared to the reluctance and cage rotors, wound rotors offer more flexible connections. It has been shown that the torque produced by this wound-loop rotor is not as big as its equivalent: nested-loop rotor [28]. However, to large-scale wind generators, a concern may arise about skin effects raising rotor resistance. In this situation, the wound rotors with multiple conductors in one slot or with multilayer windings may be attractive [29]. A more complicated double-sine wound rotor is proposed for brushless DFIMs to reduce the space harmonics of the rotor winding. It is designed to be constructed double-layer unequal-turn coils based on the principles of tooth harmonic and sinusoidal winding [30]-[31] and validated by a prototype [31]. However, it is not easy to manufacture such a complicated wound rotors. Compared to wound rotors, cage rotors have the advantages of higher fill factors and lower impedance [23]. Several different cage rotors have been built and studied [32]. Compared to the classic squirrel-cage rotor, which has poor efficiency, the nested loop rotor seems favorable because of its simplicity for cross-coupling. This construction is proposed and investigated by Broadway and Burbridge [3].

Volume 10, Issue 2
April 2021

ITEE Journal
Information Technology & Electrical Engineering

ISSN: - 2306-708X

Hybrid rotor

Hybrid rotor integrates short-circuited coils and multi-layer flux-barriers. This kind of rotor has been proposed, analyzed and used in a BDFM [33]-[34]. There is another BDFM hybrid structure rotor that uses a nested loop rotor by introducing axial ducts. These ducts also act as flow barriers by isolating adjacent magnetic circuits [35].

3. OPERATING PRINCIPLES OF BDFMs

The brushless DFIM can be thought of as two induction machines which have different pole pairs numbers, with their rotors connected together both physically and electrically. The BDFM has two modes of operation, asynchronous and synchronous and can be either singly or doubly-fed. When singly-fed, the first winding is connected to the mains (supply) and the second may be either short-circuited or open-circuited.

3.1. Asynchronous operating mode

In this operating mode, we have an asynchronous operation while doubly-fed is not desirable. Here, the BDFM behaves like two independent induction machines, each with a different synchronous speed and different pole pairs. Simple induction mode and Cascade induction mode can be obtained:

The BDFM can operate as a conventional induction machine when one winding is energized while the other control winding is in open circuit. This mode of operation is called simple induction mode.

If the open-circuited stator winding is short-circuited, the BDFIM can operate like a cascade induction machine. It is not a desirable operation mode for variable-speed wind generators. However, it is often applied in experimental measurements to evaluate rotor construction [36]-[37].

3.2. Synchronous operating mode

Synchronous operation occurs when the two stators windings induce rotor fields which interlock and produce supply frequency voltages in each other [32]. This interlocking is called cross-coupling. This mode is the desirable operating mode, and the one in which this kind of machine is typically analyzed. The cross-coupling between the two stator windings PW and CW defines the synchronous operation mode.

4. GENERAL CONSIDERATIONS

4.1. Analytical expression of the air-gap flux densities of the two stators windings

The magnetic flux density in the air-gap produced by the stator windings can be expressed by the Equations 1 and 2.

$$B_{gp}(\theta_{ag},t) = \hat{B}_{gp}\cos(\omega_p t - p_p\theta_{ag} + \phi_p) \quad (1)$$

$$B_{gc}(\theta_{ag},t) = \hat{B}_{gc}\cos(\omega_c t - p_c\theta_{ag} + \phi_c) \quad (2)$$

Where θ_{ag} is the position in the air-gap in the reference frame of the stator; ω_p and ω_c are the angular frequencies of PW and CW which are respectively equal to $2\pi f_p$ and $2\pi f_c$; and ϕ_p and ϕ_c are the initial phase angles of the PW and the CW, respectively.

With Ω_{rm} as the mechanical angular velocity of the rotor, the two previous Equations 1 and 2 can be passed in the rotor reference frame using Equation (3).

$$\theta_{ag} = \theta_{ag,r} + \Omega_{rm}t + \theta_{ag,r|t=0} \quad (3)$$

If the initial position of the rotor is assumed to be null ($\theta_{ag,r|t=0}$), then the flux density phases do not need to be changed. Using the Equations (1), (2) and (3) become (4) and (5) respectively.

$$B_{gp}(\theta_{ag,r},t) = \hat{B}_{gp}\cos\big(\omega_p - p_p\Omega_{rm})t - p_p\theta_{ag,r} + \phi_p\big) \quad (4)$$

$$B_{gc}(\theta_{ag,r},t) = \hat{B}_{gc}\cos\big(\omega_c - p_c\Omega_{rm})t - p_c\theta_{ag,r} + \phi_c\big) \quad (5)$$

Therefore, the frequencies ω_r of the rotor currents induced by the PW and CW are given by Equations (6) and (7) respectively.

$$\omega_{rp} = \omega_p - p_p\Omega_{rm} \quad (6)$$

$$\omega_{rc} = \omega_c - p_c\Omega_{rm} \quad (7)$$

To obtain cross-coupling, the frequencies of the rotor currents induced by the two stator windings PW and CW must be the same. Considering that the cosine is an even function, one can write Equation (8) as follows:

$$\omega_p - p_p\Omega_{rm} = \pm(\omega_c + p_c\Omega_{rm}) \quad (8)$$

Therefore, the synchronous angular speeds can be derived by Equations (9) and (10) as follows:

$$\Omega_{rm} = \frac{\omega_p - \omega_c}{p_p + p_c} \quad (9)$$

$$\Omega_{rm} = \frac{\omega_p + \omega_c}{p_p + p_c} \quad (10)$$

For the last two Equations, the conditions given by Equation (10) are generally preferred. In fact, this condition leads to a higher number of rotor bars [32]. Remember that in this Equation and can be negative depending on the rotation direction of the flux density they are referring to. Under this condition, the fundamental harmonics of the power and control windings will respectively interact with the first sideband harmonics of the control and power winding. Thus, the rotor ensures cross-coupling between the two stator windings.

4.2. Natural speed and slip

Natural speed

Volume 10, Issue 2
April 2021

ITEE Journal
Information Technology & Electrical Engineering

ISSN: - 2306-708X

Considering Equation (11), the natural speed of the BDFM is a mechanical speed of the machine when the Control Winding (CW) is fed with DC voltage. In which case $\omega_c = 0$.

$$\Omega_n = \frac{\omega_p}{p_p + p_c} \quad (11)$$

The natural speed of the BDFM is similar to that of the DFIM. It is the mechanical speed when there is no power passing through the power converter. Because of Equations (10) and (11), the BDFM will tend to turn slower than the synchronous speed linked to the Power Winding (PW). Thus, for low mechanical speeds, BDFMs seem to give good operating characteristics. For the wind turbine applications, this can be viewed as great advantage of the BDFM technology over the DFIM.

Slip.

In BDFMs, as in induction machines, the notion of slip can be introduced. Since there are two windings, reference [12] defines slip for each winding, as follows:

$$S_p = \frac{\omega_p - p_p \Omega_{rm}}{\omega_p} \quad (12)$$

$$S_c = \frac{\omega_c \pm p_c \Omega_{rm}}{\omega_c} \quad (13)$$

Where $\pm p_c$ depends of the windings connections of PW and CW. If the field of the CW rotates in the same direction as the one of the PW when they are both fed with 3 phases currents, then one choose "$-p_c$", if it rotates in the opposite direction one choose "$+p_c$". Considering the same phase order for both windings: the control winding slip (CW) can be given by Equation (14).

$$S_c = \frac{\omega_c - p_c \Omega_{rm}}{\omega_c} \quad (14)$$

4.3. Relationship between power winding, control winding power, and sizing of the power converter

Using an equivalent circuit, reference [12] shows that the power of the CW can be approximated from the power of the PW and the speed of the machine like as shown by Equation (15).

$$Pc = P_p \frac{\Omega_{rm}}{\Omega_n} \quad (15)$$

The converter rating can also be estimated as given in reference [38] by Equation (16).

$$S_{inv} \approx S_m \frac{\omega_{cmax}}{\omega g_{cmax}} \quad (16)$$

Where Sinv is the rating apparent power of the inverter connected to the control winding; Sm is the rated apparent power of the machine and ω_{cmax} is the maximal pulsation that must be attained by the command winding to fulfill the maximal mechanical speed needed.

5. GENERALIZED METHOD FOR APPROPRIATE CHOICE OF THE NUMBER OF POLES PAIRS

In this section, a method for an appropriate choice of the pole pairs number combinations for the BDFM is presented. This method takes into account four factors that are: number of pole combinations to avoid interaction in the stator frame, rating of the power converter, cross-coupling capability and mechanical speeds (synchronism and natural speed) to avoid.

Table 1 presents the parameters of the BDFM that will be used to evaluate the performance of the proposed method. These parameters come from study of the biggest BDFM machine built to date.

Table 1. BDFM specifications.

Rated Active Power:	Prated=20MW
Rated Synchronous Speed:	ns=60rmp
Turbine speed range:	nrm=40 to 66rmp
Frequency of grid:	f=50Hz

5.1. Conditions to be fulfilled by pole pairs to avoid direct coupling between PW and the CW

First, the number of poles of the two stators windings must be different to avoid cross-coupling through the stator iron. Therefore, the poles number must respect the following Equation (17).

$$p_p \neq p_c \quad (17)$$

Where p_p and p_c are the numbers of pole pairs of the power and control windings respectively.

As noted in [4], some combinations of number of poles can lead to an unbalanced magnetic pull. The unbalanced magnetic pull happens when the forces pulling the rotor towards the stator do not cancel each other out around the machine.

The magnetic pull can be written from the flux density of the two fundamentals in the air-gap. Using Equations (1) and (2), the flux density in the air-gap can be written by Equation (18) as follows.

$$B(\theta_{ag}, t) = \hat{B}_{gp}\, cos(\omega_p t - p_p \theta_{ag} + \phi_p) + \hat{B}_{gc}\, cos(\omega_c t - p_c \theta_{ag} + \phi_c) \quad (18)$$

The magnetic pull can be found through the integration of the Maxwell stress tensor over the perimeter of the air-gap. The Maxwell stress tensor can be expressed by equation (19) as follows.

$$\vec{\sigma} = \frac{B_n^2}{2\mu_n} \vec{u}_n \quad (19)$$

Combining Equations (18) and (19), the Maxwell stress tensor in the BDFM can be written by Equation (20).

Volume 10, Issue 2
April 2021

ITEE Journal
Information Technology & Electrical Engineering

ISSN: - 2306-708X

$$\vec{\sigma}(\theta_{ag},t)=\frac{1}{2\mu_n}[\hat{B}_{gp}^2\cos^2(\omega_p t-p_p\theta_{ag}+\phi_p)+\hat{B}_{gc}^2\cos^2(\omega_c t-p_c\theta_{ag}+\phi_c)+2\hat{B}_{gp}\hat{B}_{gc}\cos(\omega_p t-p_p\theta_{ag}+\phi_p)\cos(\omega_c t-p_c\theta_{ag}+\phi_c)]\vec{u}_n(\theta_{ag}) \quad (20)$$

The projection of $\vec{u}_n(\theta_{ag})$ on an axis can be written $\cos(\theta_{ag}+\phi)]\vec{u}_{axis}$; where ϕ depends on the direction of the projection. So, the force of the magnetic pull projected on an axis can then be written as follows (21):

$$\vec{F}_{mp}(t)=\int_0^{2\pi}\frac{1}{2\mu_0}[\hat{B}_{gp}^2\cos^2(\omega_p t-p_p\theta_{ag}+\phi_p)+\hat{B}_{gc}^2\cos^2(\omega_c t-p_c\theta_{ag}+\phi_c)+2\hat{B}_{gp}\hat{B}_{gc}\cos(\omega_p t-p_p\theta_{ag}+\phi_p)\cos(\omega_c t-p_c\theta_{ag}+\phi_c)]\cos(\theta_{ag}+\phi)d\theta_{ag}\vec{u}_{axis} \quad (21)$$

Considering that: $\cos^2(x)=\frac{1}{2}+\frac{\cos(2x)}{2}$ and $\cos(x)\cos(y)=\frac{1}{2}(\cos(x+y)+\cos(x-y))$, Equation (21) becomes (22).

$$\vec{F}_{mp}(t)=\frac{1}{2\mu_0}\int_0^{2\pi}[\hat{B}_{gp}^2\cos^2(\omega_p t-p_p\theta_{ag}+\phi_p)+\hat{B}_{gc}^2\cos^2(\omega_c t-p_c\theta_{ag}+\phi_c)+2\hat{B}_{gp}\hat{B}_{gc}\cos(\omega_p t-p_p\theta_{ag}+\phi_p)\cos(\omega_c t-p_c\theta_{ag}+\phi_c)]\cos(\theta_{ag}+\phi)d\theta_{ag}\vec{u}_{axis} \quad (22)$$

Equation (22) shows that the total magnetic pull force will be equal to zero if only and if: $|2p_p|\neq 1$, $|2p_c|\neq 1$, $|p_p+p_c|\neq 1$ and $|p_p-p_c|\neq 1$. Since p_p and p_c are both positive integers, the combination that can create an unbalanced magnetic pull from the fundamental harmonics are a combination such as: $p_p=p_c\pm 1$.

Thus, for an appropriate design of BDFM, p_p and p_c must be chosen such as:

$$\begin{cases}p_p\neq p_c\\ p_p\neq p_c\pm 1\end{cases} \quad (23)$$

5.2. Number of poles and rating of the power converter

As for a DFIM, the choice of the total number of poles of a BDFM will impact the minimum rating of the power converter.

The power converter is linked to the control winding so its rating can be defined from the maximum power and related power factor of this winding (24).

$$S_{pc}=\frac{P_{cmax}}{\cos\phi_{cmax}} \quad (24)$$

S_{pc} is the apparent rated power of the power converter; P_{cmax} is the maximum active power of the control winding; $\cos(\phi_{cmax}$ is the power factor of the control winding when the maximum active power is reached.

From the equivalent circuit, it is possible under certain assumptions to simplify the expressions of the active and reactive powers of the power and control windings. With these simplifications, the active power of the control winding can be expressed from the active power of the power winding and the ratio of pulsations as shown in Equation (25). Such a development can be found in [39].

$$P_c\approx P_p\frac{\omega_c}{\omega_g} \quad (25)$$

The rated active power of the BDFM is the sum of the rated powers of the power and control windings. It is given by Equation (26).

$$P_{rated}=P_{c\ rated}+P_{p\ rated} \quad (26)$$

P_{rated} is the rated active power of the BDFM; $P_{c\ rated}$ is the rated active power of the control winding; $P_{p\ rated}$ is the rated active power of the power winding. Replacing $P_{p\ rated}$ in Equation (26) by its expression from Equation (25) leads to Equation (27).

$$P_{c\ rated}=\frac{P_{rated}}{1+\frac{\omega_g}{\omega_c}} \quad (27)$$

To minimize the sizing of the power converter connected to the control winding, it is important to limit the rated power of the control winding $P_{c\ rated}$. Equation (27) shows that the active power of the control winding depends to the total active power of the machine and to the ratio of electrical pulsations of the two stator windings. The electrical pulsation of the power winding being equal to the pulsation of the grid (50Hz or 60Hz). So, with Equation (27), it is easy to see that a design that minimizes the rated power of the control winding $(P_{c\ rated})$ will be a design that also minimizes its pulsation ω_c. It is also preferable for the control winding pulsation to be positive: the two magnetic fields of the two stator windings will then have the same rotation direction and their power will add up and not subtract from each other.

Considering that rotor speed varies between n_{rmmin} and n_{rmmax} and the pulsation of the grid is f, to meet the precedent criteria, p_p and p_c must be set as given by Equations (28) and (29).

$$\frac{2\pi f}{p_p+p_c}<\frac{2\pi n_{rmmin}}{60} \quad (28)$$

$$\frac{2\pi f}{p_p+p_c}>\frac{2\pi n_{rmmax}}{60} \quad (29)$$

Volume 10, Issue 2
April 2021

ITEE Journal
Information Technology & Electrical Engineering

ISSN: - 2306-708X

These Equations can be rewritten as follows:

$$p_p + p_c \succ \frac{60f}{n_{rmmin}} \quad (30)$$

$$p_p + p_c \prec \frac{60f}{n_{rmmax}} \quad (31)$$

Using the parameters presented in table 1, we obtain the following conditions:

$$p_p + p_c \succ 75 \quad (32)$$

$$p_p + p_c \prec 45 \quad (33)$$

Using the parameters given in the table 1, it appears that the total power of the machine is not constant over the range of speed. Figure 2 shows the total power of the machine and the approximative power of each winding using the parameters from table 1, and Equations (10), (25) and (26) for different number of poles.

In this figure 2, we observe that when the sum of the number of pole pairs is such as $p_p + p_c \prec 45$, the control winding always working against the power winding. One winding generates power and the other consumes power. In the Equations, this will be translated by a "negative" control winding pulsation: $\omega_c \prec 0$. And when the number of pole pairs is such as $p_p + p_c \succ 75$, the two windings work in the same direction: the stator windings generate and consume power simultaneously. In the Equations, this will be translated by a "positive" control winding pulsation: $\omega_c \succ 0$.

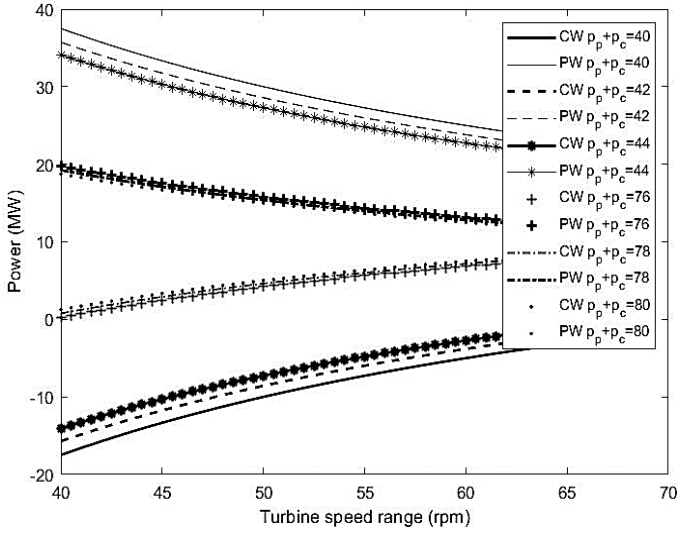

Figure 2. Active Power depending on the total number of pole pairs ($p_p + p_c$) and the mechanical speed of the rotor.

With figure 2, it is then easy to see that to minimize the sizing power winding, the control winding and the power converter, the natural speed of the BDFM should be set below the lowest speed of the machine. This results in a sum of number of poles a bit above seventy-five. In the following part of the specifications of the BDFM, we will remember using Fig. 2 and 3 that the possible sum of pole pairs can be setting as: $p_p + p_c = 76$, $p_p + p_c = 78$ or $p_p + p_c = 80$.

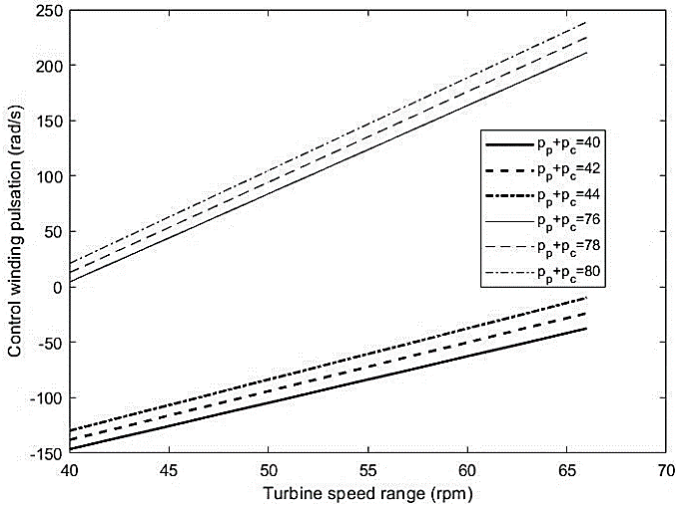

Figure 3. Control winding pulsation depending on the total number of pole pairs ($p_p + p_c$) and the mechanical speed of the rotor.

5.3. Cross-coupling capability depending on the number of poles

The choices of p_p and p_c can be determined by trying to maximize the cross-coupling factor of the stator windings through the rotor. According to geometry considerations (in [38]), this cross-coupling factor is given by Equation (34) below.

$$k_{pc} \propto sin\left(p_p \frac{\theta_R/\theta_{Rmax}}{2}\right) sin\left(p_c \frac{\theta_R/\theta_{Rmax}}{2}\right) \quad (34)$$

Where k_{pc} is the cross-coupling factor, θ_R is the rotor loop span angle and θ_{Rmax} is the maximum rotor loop span angle.

The rotor loop span angle θ_R is the angle between the two bars of the external loop of each nest. The maximum value the rotor loop span angle can take can be expressed using Equation (35).

$$\theta_{R\,max} = \frac{360}{p_p + p_c} \quad (35)$$

The higher cross-coupling factor between the two stator windings is, the better the BDFM will work. Because of the expression of the cross-coupling factor in Equation (34), for a given total number of pole pairs $p_p + p_c$, different choices of p_p and p_c will not all lead to a good working BDFM.

The best total numbers of pole pairs $p_p + p_c$ for the specification of the BDFM has been previously estimated to be 76, 78, or 80 using Figure 3. Thus, it is interesting to compare the potential cross-coupling factors of all the possible combinations of p_p and p_c according to Equation (34). We should notice that Equation (34) is symmetrical for p_p and p_cThus, if then if p_p and p_c are permuted, the cross-coupling factor is not impacted.

Volume 10, Issue 2
April 2021

ITEE Journal
Information Technology & Electrical Engineering

ISSN: - 2306-708X

As it can be seen the high cross-coupling factors are achieved when the values of p_p and p_c are close. Of course, $p_p = p_c$ gives the highest potential cross-coupling factor. But $p_p = p_c$ is forbidden to avoid cross-coupling in the stator reference frame as reminded in Equation (23). The combinations of p_p and p_c where $p_p = p_c \pm 1$ also give very good cross-coupling capabilities. However, these combinations will create unbalanced magnetic pull as it was explained (see Equation (23)). These are also forbidden combinations.

Is still possible to select the combinations of p_p and p_c that can give a potential high cross-coupling factor. If the threshold is set at 90% of the highest cross-coupling factor, for $p_p + p_c = 76$, there are 7 possible combinations which are: $p_c = 39$ and $p_p = 37$; $p_c = 40$ and $p_p = 36$; $p_c = 41$ and $p_p = 35$; $p_c = 42$ and $p_p = 34$; $p_c = 43$ and $p_p = 33$; $p_c = 44$ and $p_p = 32$ and finally $p_c = 45$ and $p_p = 31$.

Of course, as already said, the theoretical maximum cross-coupling factor remains identical even if the number of pole pairs of the control and power winding are permuted. Thus, the previous seven combinations can be extended to fourteen combinations. To minimize the number of stator teeth, it is important to select a combination with a high Greatest Common Divisor (GCD) between the pole pairs of the two stator windings. This condition eliminates many combinations.

The same logic can be applied to $p_p + p_c = 78$ and to $p_p + p_c = 80$. The results of all potential pole configurations and the related GCD to the pole pairs of their two windings are given in table 2.

From table 2, one pole configuration leads to highest Great Common Divisor than all the other configurations. It is the couple: $p_p = 32$, $p_c = 48$; so $GCD(32,48) = 16$. The same result is obtained if the number of poles of the two stator windings is permuted. In the following part, the two poles configurations: $p_p = 32$ and $p_c = 48$, and $p_c = 48$ and $p_p = 32$, will be further investigated.

Table 2. Different possible configurations of pole pairs with the GCD between the pole pairs of the two stator windings

$p_p+p_c=76$		$p_p+p_c=78$		$p_p+p_c=80$	
Pole Configuration	GCD	Pole Configuration	GCD	Pole Configuration	GCD
pp=37, pc=39	1	pp=38, pc=40	2	pp=39, pc=41	1
pp=36, pc=40	4	pp=37, pc=41	1	pp=38, pc=42	2
pp=35, pc=41	1	pp=36, pc=42	6	pp=37, pc=43	1
pp=34, pc=42	2	pp=35, pc=43	1	pp=36, pc=44	4
pp=33, pc=43	1	pp=34, pc=44	2	pp=35, pc=45	5
pp=32, pc=44	4	pp=33, pc=45	3	pp=34, pc=46	2
pp=31, pc=45	1	pp=32, pc=46	2	pp=33, pc=47	1
		pp=31, pc=47	1	pp=32, pc=48	16

5.4. Mechanical speeds to avoid: synchronous speed and natural speed

As it can be seen from Equations (12) and (14), a slip can be defined for each winding. When one of the slips becomes null, the induced rotor currents from the related stator winding becomes null too. Without these induced rotor currents, the stator windings are not interacting each other through the rotor: there is no more cross-coupling.

From Equations (12) and (14), it is possible to deduce the synchronism speeds for which the cross-coupling effect of the BDFM disappears:

$$n_{sp} = \frac{60\omega_p}{2\pi p_p} \quad (36)$$

$$n_{sc} = \frac{60\omega_c}{2\pi p_c} \quad (37)$$

n_{sp} and n_{sc} are the synchronism speeds of the power and control windings respectively (in rmp). ω_p and ω_c are the electrical pulsations of the power and control windings respectively (in rad/s).

Under cross-coupling, the mechanical speeds and pulsations of the windings are linked by equation (10). The pulsation of the control winding to reach the minimal and maximal speed of the interval can be computed using Equation (38).

$$\omega_c = 2\pi f_c = \frac{2\pi}{60} n_{rm}(p_p + p_c) - \omega_p \quad (38)$$

In table 3, the feeding frequency of the control winding is computed for the minimum and maximum mechanical speeds of the rotor according to Equation (38).

Table 3. Frequency of the control winding for different speed of the BDFM

Pole configuration	fcmin (nrm=40 rmp)	fcmin (nrm=66 rmp)	fcmin (nrm=60 rmp)
pp=32, pc=48	3.3Hz	38Hz	30Hz
pp=48, pc=32	3.3Hz	38Hz	30Hz

Combining Equations (36), (37) and (38), it is possible to write the forbidden speeds at which there is no more cross-coupling because one of the winding does not induce current anymore in the rotor of the BDFM. The forbidden mechanical speeds can be written according to Equation (39):

Volume 10, Issue 2
April 2021

ITEE Journal
Information Technology & Electrical Engineering

ISSN: - 2306-708X

$$\begin{cases} n_{sp} = \dfrac{60\omega_p}{2\pi p_p} \\ n_{sc} = \dfrac{60\left(\frac{2\pi}{60} n_{rm}(p_p+p_c)-\omega_p\right)}{2\pi p_c} \\ n_n = \dfrac{60\omega_p}{2\pi(p_c+p_c)} \end{cases} \quad (39)$$

In Equation (39), the synchronism speed of the power winding and the natural speed do not depend on the mechanical speed of the rotor. In table 4, the synchronism speed of the power winding and the natural speed of the BDFM are computed for the two poles configurations selected.

Table 4. Forbidden speeds for two different pole configurations

Pole configuration	n_{sp}	n_n
p_p=32, p_c=48	93.75 rmp	37.5 rmp
p_p=48, p_c=32	62.5 rmp	37.5 rmp

With this table 4, it is possible to eliminate the pole configuration $p_p = 48$, $p_c = 32$ as a potential solution for the design of BDFM. Indeed, with this pole configuration, the forbidden synchronous speed of the power winding is at $62.5rmp$, which is in the middle of the speed range in the specifications of our BDFM from 40 to $66rmp$ (specifications given in table 1).

But table 4 does not give any information about the forbidden synchronous speed of the control winding. According to Equation (39), the synchronous speed varies with the mechanical speed. Using this Equation, it is possible to plot the forbidden speeds of the BDFM as a function of the mechanical speed of the rotor.

When the rotor speed will vary between n_{rmmin} and n_{rmmax} (40 to 66 *rmp*), the synchronous speed of the control winding will vary linearly between n_{scmin} and n_{scmax}. The case of a loss of the cross-coupling due to a forbidden speed will arise if one of the forbidden speed curves crosses the mechanical.

As it can be seen in table 4 and figure 4, in the range of operation between $40rmp$ and $66rmp$, the BDFM with $p_p = 32$and $p_c = 48$ does not have any problem with a loss of the cross-coupling due to a forbidden speed. However, considering fig. 5, the BDFM with $p_p = 48$and $p_c = 32$ not work in cross-coupling in all the range of operation speed, because we loss the cross-coupling at $n_{rm} = 62.5rmp$.

This new generalized method for an appropriate choice of pole-pairs combinations can be summarize in the flowchart presented in figure 6.

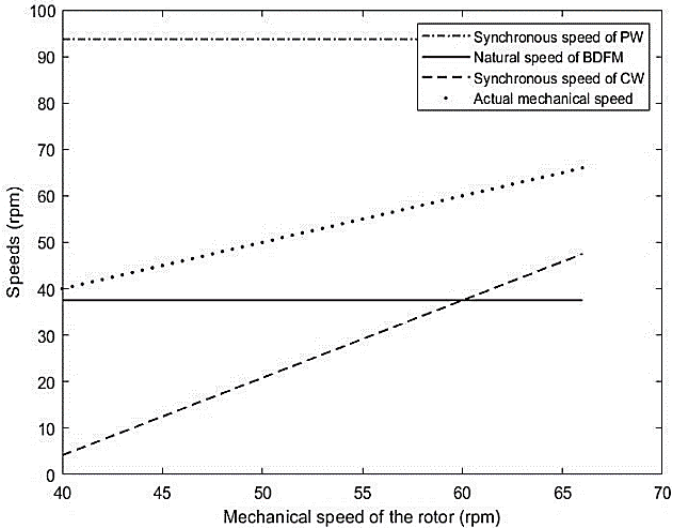

Figure 4. Mechanical and forbidden speeds as a function of the mechanical speed for pp=32, pc=48.

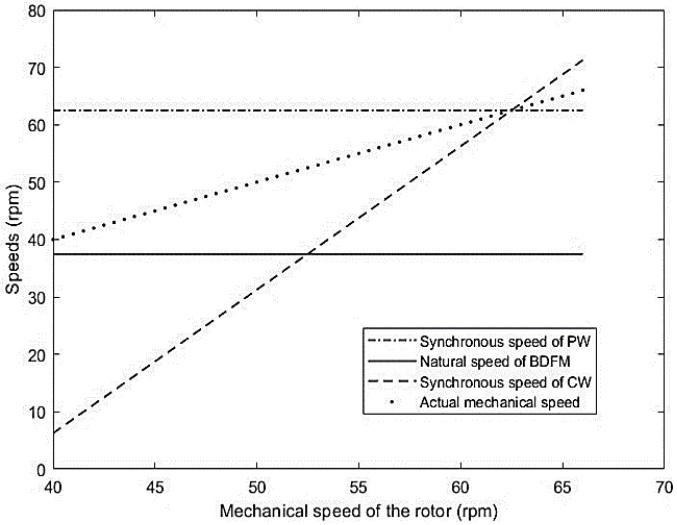

Figure 5. Mechanical and forbidden speeds as a function of the mechanical speed for pp=48, pc=32.

As can been seen in table 5, using the flowchart given in figure 6, we can successfully obtained the same number of pole pairs combinations for every type of machine presented in [40-45].

Table 5. Generalized method vs ab initio

References	Characteristics	Pole pairs
[40-43] This work	Frame size: D400 Rated power: 250kw Speed range: [320-680] rpm	Pp=4, Pc=8
[44-45] This work	Frame size: D180 Rated power: 7.8 kw Speed range: [335-997.5] rpm	Pp=2, Pc=4

6. POTENTIALS USES OF THESE RESULTS

As mentioned above, the choice of the number of pole pairs for a good exploitation of the performance of a BDFM is of great importance. This work contributes to the optimal design process of the BDFM by proposing a generalized method which makes it possible to make a favorable choice of the number of pole pairs of this type of machine. Indeed, during the BDFM design phase, this method will, under the constraint of several factors, lead to a combination of a number of pole

Volume 10, Issue 2
April 2021

ITEE Journal
Information Technology & Electrical Engineering

ISSN: - 2306-708X

pairs having a good cross-coupling factor with a synchronism speed located in the operating range of the machine while minimizing the power consumed by the power converter.

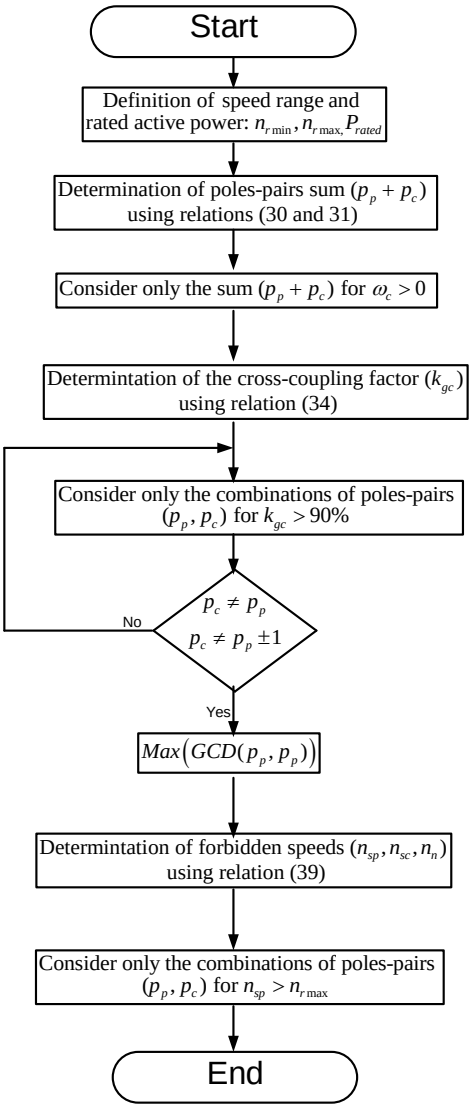

Figure 6. Flowchart of generalized method for appropriate choice of pole number combinations.

7. CONCLUSION

In this work, we proposed a generalized method for an appropriate choice of pole number combinations for the design of a Brushless Doubly-Fed Machines. The choice of number of poles to give a desired natural speed is the first and most important point in the design process of all BDFM, but the process to define the optimal number of poles for BDFM was not yet well established. After taking into account the active power of the control winding, the cross-coupling factor, the symmetry and the forbidden speeds that prevent the cross-coupling, only one pole configuration was successfully selected for our project of $20\ MW$ (Table 1): $p_p = 32$ and $p_c = 48$. For projects with other specifications, especially projects rotating a bit faster, there might be more than one pole configurations that meet all the criteria. In this case, we have suggested that additional criterion can further the selection: the number of pole pairs of the control winding must be greater than the power winding pole pairs. This criterion can be verified in the literature in where we have $p_p = 1$ and $p_c = 3$ in [46], $p_p = 4$ and $p_c = 6$ in [46], [47], $p_p = 2$ and $p_c = 4$ in [40], [47]-[49] for the $250\ kW$ BDFM. This work has shown the possibility to use a new definition process to choose the optimal number of poles for the BDFM and to obtain the results already proposed in the literature.

REFERENCES

[1.] F. Blazquez, C. Veganzones, D. Ramirez, C. Platero, "Characterization of the rotor magnetic field in a brushless doubly-fed induction machine", IEEE Transactions on Energy Conversion 24 (3) (2009) 599–607.

[2.] H. Liu, L. Xu, "Design and performance analysis of a doubly excited brushless machine for wind power generator application", in: The 2nd International Symposium on Power Electronics for Distributed Generation Systems, IEEE, 2010, pp. 597–601.

[3.] F. Lydall, et al., "Improvement in polyphase induction motors", British Patent 16839.

[4.] L. J. Hunt, "A new type of induction motor," Journal of the Institution of Electrical Engineers 39 (186) (1907) 648–667.

[5.] L. J. Hunt, "The "cascade" induction motor", Journal of the Institution of Electrical Engineers 52 (230) (1914) 406–426. doi:10.1049/jiee-1.1914.0031.

[6.] F. Creedy, "Some developments in multi-speed cascade induction motors", Journal of the Institution of Electrical Engineers 59 (301) (1921) 511–532. doi:10.1049/jiee-1.1921.0036.

[7.] A. R. W. Broadway, L. Burbridge, "Self-cascaded machine: a low-speed motor or high-frequency brushless alternator", Proceedings of the Institution of Electrical Engineers 117 (7) (1970) 1277–1290. doi:10.1049/piee.1970.0247.

[8.] A. Broadway, "Cageless induction machine", in: Proceedings of the Institution of Electrical Engineers, Vol. 118, IET, 1971, pp. 1593–1600.

[9.] A. Broadway, B. Cook, P. Neal, "Brushless cascade alternator", in: Proceedings of the Institution of Electrical Engineers, Vol. 121, IET, 1974, pp. 1529–1535.

[10.] A. Wallace, R. Spee, G. Alexander, "Adjustable speed drive and variable speed generation systems with reduced power converter requirements", in: ISIE'93-Budapest: IEEE International Symposium on Industrial Electronics Conference Proceedings, IEEE, 1993, pp. 503–508.

[11.] C. S. Brune, R. Spee, A. K. Wallace, "Experimental evaluation of a variable-speed, doubly-fed wind-power

generation system", IEEE Transactions on Industry Applications 30 (3) (1994) 648–655.

[12.] R. A. McMahon, X. Wan, E. Abdi-Jalebi, P. J. Tavner, P. C. Roberts, M. Jagiela, "The bdfm as a generator in wind turbines", in: 2006 12th International Power Electronics and Motion Control Conference, IEEE, 2006, pp. 1859–1865.

[13.] S. Shao, E. Abdi, R. McMahon, "Operation of brushless doubly-fed machine for drive applications".

[14.] H. Arabian-Hoseynabadi, H. Oraee, P. Tavner, "Failure modes and effects analysis (fmea) for wind turbines", International Journal of Electrical Power & Energy Systems 32 (7) (2010) 817–824.

[15.] T. Logan, J. Warrington, S. Shao, R. McMahon, "Practical deployment of the brushless doubly-fed machine in a medium scale wind turbine", in: 2009 International Conference on Power Electronics and Drive Systems (PEDS), IEEE, 2009, pp. 470–475.

[16.] S. Williamson, A. Ferreira, "Generalised theory of the brushless doubly-fed machine. part 2: Model verification and performance", IEE Proceedings-Electric Power Applications 144 (2) (1997) 123–129.

[17.] P. Roberts, R. McMahon, P. Tavner, J. Maciejowski, T. Flack, "Equivalent circuit for the brushless doubly fed machine (bdfm) including parameter estimation and experimental verification", IEE Proceedings-Electric Power Applications 152 (4) (2005) 933–942.

[18.] Y. Liao, "Design of a brushless doubly-fed induction motor for adjustable speed drive applications", in: IAS'96. Conference Record of the 1996 IEEE Industry Applications Conference Thirty-First IAS Annual Meeting, Vol. 2, IEEE, 1996, pp. 850–855.

[19.] X. Wang, R. McMahon, P. Tavner, "Design of the brushless doubly-fed (induction) machine", in: 2007 IEEE International Electric Machines & Drives Conference, Vol. 2, IEEE, 2007, pp. 1508–1513.

[20.] F. Runcos, R. Carlson, N. Sadowski, P. Kuo-Peng, H. Voltolini, "Performance and vibration analysis of a 75 kw brushless double-fed induction generator prototype", in: Conference Record of the 2006 IEEE Industry Applications Conference Forty-First IAS Annual Meeting, Vol. 5, IEEE, 2006, pp. 2395–2402.

[21.] S. Williamson, A. Ferreira, A. Wallace, "Generalised theory of the brushless doubly-fed machine. part 1: Analysis", IEE Proceedings-Electric Power Applications 144 (2) (1997) 111–122.

[22.] F. Runcos, R. Carlson, A. Oliveira, P. Kuo-Peng, N. Sadowski, "Performance analysis of a brushless double fed cage induction generator", in: Nordic Wind Power Conference, Vol. 1, Chalmers University of Technology, 2004.

[23.] L. Xu, F. Wang, "Comparative study of magnetic coupling for a doubly fed brushless machine with reluctance and cage rotors", in: IAS'97. Conference Record of the 1997 IEEE Industry Applications Conference Thirty-Second IAS Annual Meeting, Vol. 1, IEEE, 1997, pp. 326–332.

[24.] F. Wang, F. Zhang, L. Xu, "Parameter and performance comparison of doubly fed brushless machine with cage and reluctance rotors", IEEE Transactions on Industry Applications 38 (5) (2002) 1237–1243.

[25.] A. M. Knight, R. E. Betz, W. K. Song, D. G. Dorrell, "Brushless doubly-fed reluctance machine rotor design", in: 2012 IEEE Energy Conversion Congress and Exposition (ECCE), IEEE, 2012, pp. 2308–2315.

[26.] A. M. Knight, R. E. Betz, D. G. Dorrell, "Design and analysis of brushless doubly fed reluctance machines", IEEE Transactions on Industry Applications 49 (1) (2012) 50–58.

[27.] S. Kunte, M. Bhawalkar, N. Gopalakrishnan, Y. Nerkar, "Design and analysis of brushless doubly fed reluctance machine suitable for wind generation applications", in: 2015 18th International Conference on Electrical Machines and Systems (ICEMS), IEEE, 2015, pp. 2082–2088.

[28.] R. McMahon, P. Tavner, E. Abdi, P. Malliband, D. Barker, "Characterising brushless doubly fed machine rotors", IET Electric Power Applications 7 (7) (2013) 535–543.

[29.] Y. Guo, X. Wang, J. G. Zhu, H. Lu, "Development of a wound rotor brushless doubly fed machine based on slot mmf harmonics", in: 2008 IEEE Industry Applications Society Annual Meeting, IEEE, 2008, pp. 1–5.

[30.] F. Xiong, X. Wang, "Design of a low-harmonic-content wound rotor for the brushless doubly fed generator", IEEE Transactions on Energy Conversion 29 (1) (2013) 158–168.

[31.] F. Xiong, X. Wang, "Design and performance analysis of a brushless doubly-fed machine for stand-alone ship shaft generator systems", in: 2011 International Conference on Electrical and Control Engineering, IEEE, 2011, pp. 2114–2117.

[32.] P. C. Roberts, "Study of brushless doubly-fed (induction) machines: contributions in machine analysis, design and control", Ph.D. thesis, University of Cambridge (2005).

[33.] F. Zhang, L. Zhu, S. Jin, X. Su, S. Ademi, W. Cao, "Controller strategy for open-winding brushless doubly fed wind power generator with common mode voltage

elimination", IEEE Transactions on Industrial Electronics 66 (2) (2018) 1098–1107.

[34.] F. Zhang, G. Jia, Y. Zhao, Z. Yang, W. Cao, J. L. Kirtley, "Simulation and experimental analysis of a brushless electrically excited synchronous machine with a hybrid rotor", IEEE Transactions on Magnetics 51 (12) (2015) 1–7.

[35.] S. Abdi, E. Abdi, A. Oraee, R. McMahon, "Optimization of magnetic circuit for brushless doubly fed machines", IEEE Transactions on Energy Conversion 30 (4) (2015) 1611–1620.

[36.] P. Roberts, R. McMahon, P. Tavner, J. Maciejowski, T. Flack, X. Wang, "Performance of rotors for the brushless doubly-fed (induction) machine (bdfm)", in: The 16th International Conference on Electrical Machines, Cracow, Poland, Vol. 1, 2004, pp. 450–455.

[37.] P. Tavner, R. McMahon, P. Roberts, E. Abdi-Jalebi, X. Wang, M. Jagiela, T. Chick, "Rotor design & performance for a bdfm", in: Proc. of the XVII international conference on electrical machines, 2006.

[38.] M. S. Boger, A. K. Wallace, R. Spee, "Investigation of appropriate pole number combinations for brushless doubly fed machines applied to pump drives", IEEE Transactions on Industry Applications 32 (1) (1996) 189–194. doi:10.1109/28.485831.

[39.] F. J. P. Lobo, "Modélisation, conception et commande d'une machine asynchrone sans balais doublement alimentée pour la génération à vitesse variable", PhD. thesis (2003).

[40.] E. Abdi, R. McMahon, P. Malliband, S. Shao, M. E. Mathekga, P. Tavner, S. Abdi, A. Oraee, T. Long, M. Tatlow, "Performance analysis and testing of a 250 kw medium-speed brushless doubly-fed induction generator", IET Renewable Power Generation 7 (6) (2013) 631–638.

[41.] R. McMahon, P. Roberts, X. Wang, P. Tavner, "Performance of bdfm as generator and motor", IEE Proceedings-Electric Power Applications 153 (2) (2006) 289–299.

[42.] S. Abdi, E. Abdi, A. Oraee, R. McMahon, "Equivalent circuit parameters for large brushless doubly fed machines (bdfms)", IEEE Transactions on Energy Conversion 29 (3) (2014) 706–715.

[43.] S. Abdi Jalebi, E. Abdi, A. Oraee, R. McMahon, "Optimisation of magnetic circuit for brushless doubly fed machines".

[44.] E. Abdi, X. Wang, S. Shao, R. A. McMahon, P. Tavner, "Performance characterisation of brushless doubly-fed generator", in: 2008 IEEE industry applications society annual meeting, IEEE, 2008, pp. 1–6.

[45.] S. Tohidi, "Analysis and simplified modelling of brushless doubly-fed induction machine in synchronous mode of operation", IET Electric Power Applications 10 (2) (2016) 110–116.

[46.] T. D. Strous, X. Wang, H. Polinder, J. B. Ferreira, "Finite element based multi-objective optimization of a brushless doubly-fed induction machine", in: 2015 IEEE International Electric Machines & Drives Conference (IEMDC), IEEE, 2015, pp. 1689–1694.

[47.] R. Resmi, C. A. Agoram, P. Adithya, V. Vanitha, "Design and analysis of brushless doubly fed induction generator", Procedia Technology 21 (2015) 604–610.

[48.] H. Gorginpour, H. Oraee, R. A. McMahon, "A novel modeling approach for design studies of brushless doubly fed induction generator based on magnetic equivalent circuit", IEEE Transactions on Energy Conversion 28 (4) (2013) 902–912.

[49.] R. McMahon, P. Tavner, E. Abdi, P. Malliband, D. Barker, "Characterising rotors for brushless doubly-fed machines (bdfm)", in: The XIX International Conference on Electrical Machines-ICEM 2010, IEEE, 2010, pp. 1–6.

AUTHOR PROFILE

KENDEG ONLA Clement junior was born in Mbongo-Ndonga in Cameroon, on February 11, 1994. He received the B.Eng. degree in electrical engineering from Higher Institute of Technology and Industrial Design, Douala, Cameroon, in 2015 and the M.Sc. degree in Electronics, Electrical Engineering and Automation (EEA) from Ngaoundere University, Cameroon, in 2018.He is currently working toward the Ph.D. degree in electrical machines design, modeling, control and optimization at Ngaoundere University, Cameroon. His research interests include electrical machines and drives for renewable energy power generation, electrical transformers and the modeling of electromagnetic devices.